Two-Photon Fluorescent Probes

DOI: 10.1002/ange.201002907

Dual-Color Imaging of Sodium/Calcium Ion Activities with Two-Photon Fluorescent Probes**

Hyung Joong Kim, Ji Hee Han, Mi Kyung Kim, Chang Su Lim, Hwan Myung Kim, and Bong Rae Cho**

Calcium ions act as a ubiquitous second messenger that controls various functions in cells.[1,2] In mammallian cells, the cytosolic free Ca^{2+} concentration ($[Ca^{2+}]_c$) is maintained at about 0.1 μM by the coordinated actions of various calcium ion channels and transporters,[1,2] whereas the extracellular Ca^{2+} concentration is greater than 1 mM. The near-membrane Ca^{2+} concentration ($[Ca^{2+}]_m$) is much higher than $[Ca^{2+}]_c$ and can reach values of greater than 100 μM upon activation.[2] The domains with high $[Ca^{2+}]_m$ are the key regions that regulate physiological processes, such as exocytosis, ion-channel activities, and sensory transductions.[2]

Na^+/Ca^{2+} exchange is an important activity that is relevant to Ca^{2+} homeostasis,[2,3] and the simultaneous detection of Na^+ and Ca^{2+} near the cell membrane is crucial to understanding this process. Two-photon microscopy (TPM), a technique that utilizes two photons of lower energy for excitation,[4] is an ideal tool to study Na^+/Ca^{2+} exchange. Combined with appropriate TP probes, TPM can visualize biological events within live cells and deep inside intact tissues (> 500 μm) for an extended periods of time.[5] Very recently, we reported TP probes for $[Ca^{2+}]_m$ (ACaL) and intracellular free Na^+ ($[Na^+]_i$) (ANa1) that can detect $[Ca^{2+}]_m$ and $[Na^+]_i$, respectively, in live cells and intact tissues by TPM (Scheme 1).[6,7] However, the dissociation constant of ACaL ($K_d = 41$ nM) was too small to detect $[Ca^{2+}]_m$ at the 100 μM level. Moreover, simultaneous detection of the two ions was not possible because the emission bands from the two probes appeared in the same wavelength range. Overcoming these problems requires the development of an efficient TP probe for $[Ca^{2+}]_m$ that shows K_d of about 100 μM and emits TP excited fluorescence (TPEF) at a wavelength different from that of ANa1. We have therefore designed a new TP probe for $[Ca^{2+}]_m$ (BCaM, Scheme 1) derived from 2-(2′-morpholino-2′-oxoethoxy)-*N*,*N*-bis(hydroxycarbonylmethyl)aniline (MOBHA) as the Ca^{2+} receptor and 6-(benzo[*d*]oxazol-2′-yl)-2-(*N*,*N*-dimethylamino)naphthalene as the reporter. Herein, we show that, by using BCaM and ANa1, we can simultaneously detect $[Ca^{2+}]_m$ and $[Na^+]_i$ in live cells and tissues at depths of more than 100 μm for lengthy periods of time without photobleaching problems.

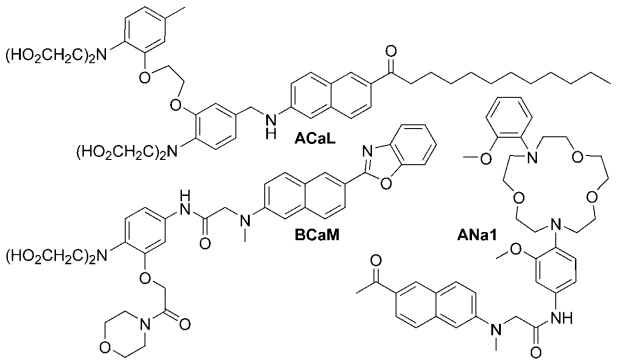

Scheme 1. Structures of ACaL, BCaM, and ANa1.

The preparation of BCaM is described in the Supporting Information. The water solubility of BCaM was approximately 5 μM, which was sufficient to stain the cells (Supporting Information, Figure S1). The absorption and emission spectra of BCaM showed gradual red shifts with increasing solvent polarity (Supporting Information, Figure S2). The shifts were greater for the fluorescence emission (40 nm) than for the absorption spectra (5 nm), but not as sensitive as ANa1 to the polarity of the environment ($\Delta\lambda_{fl} = 40$ vs 79 nm).[7] Moreover, the emission band of BCaM was well separated from that of ANa1 (Figure 1 d).

When Ca^{2+} was added to BCaM in 3-(*N*-morpholino)propanesulfonic acid (MOPS) buffer solution (30 mM, 100 mM KCl, pH 7.2), the fluorescence intensity increased dramatically as a function of metal ion concentration (Figure 1 a), which is probably due to the blocking of the photoinduced electron transfer (PET) process by the complexation with the metal ions. A nearly identical result was observed in the TP process (Supporting Information, Figure S3). The fluorescence enhancement factors ($FEF = (F - F_{min})/F_{min}$) of BCaM determined for the one- and two-photon processes in the presence of 2.5 mM Ca^{2+} was 13 and 14, respectively. It is worth noting that the BCaM/Ca^{2+} complex shows the largest fluorescent quantum yield ($\Phi = 0.98$) reported to date among Ca^{2+} ion probes (Supporting Information, Table S1). The

[*] H. J. Kim,[+] M. K. Kim, Prof. H. M. Kim
Division of Energy Systems Research, Ajou University
Suwon, 443-749 (Korea)
Fax: (+82) 31-219-1615
E-mail: kimhm@ajou.ac.kr
J. H. Han,[+] C. S. Lim, Prof. B. R. Cho
Department of Chemistry, Korea University
1-Anamdong, Seoul, 136-701 (Korea)
Fax: (+82) 2-3290-3544
E-mail: chobr@korea.ac.kr
[+] These two authors contributed equally to this work.

[**] This work was supported by the National Research Foundation (NRF) grants funded by the Korean Government (No. 2009-0065783 and 2009-0083078) and Priority Research Centers Program through the NRF funded by the Ministry of Education, Science, and Technology (2009-0093826).
Supporting information for this article is available on the WWW under http://dx.doi.org/10.1002/anie.201002907.

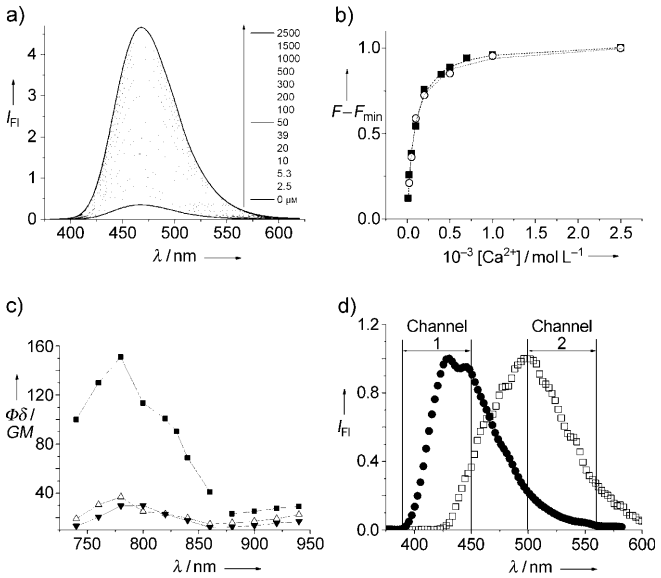

Figure 1. a) One-photon fluorescence spectra of 1 μM BCaM (30 mM MOPS, 100 mM KCl, pH 7.2) in the presence of free Ca^{2+} (0–2.5 mM). b) One-photon fluorescence titration of BCaM in LUVs composed of raft mixture (■) and two-photon fluorescence titration in HeLa cells (○) in the presence of various concentrations of free Ca^{2+} ions (0–2.5 mM). c) Two-photon action spectra of BCaM (■), Fura-2 (△), and Calcium Green (▼) in the presence of excess free Ca^{2+} ions. d) Normalized emission spectra of BCaM (●) and ANa1 (□) in HeLa cells.

dissociation constants (K_d^{OP} and K_d^{TP}) of BCaM for the one- and two-photon processes were calculated from the fluorescence titration curves (Supporting Information, Figure S3).[6,7] The titration curves fitted well with a 1:1 binding model and the Hill plots were linear with a slope of 1.0, indicating 1:1 complexation between the probe and Ca^{2+} (Supporting Information, Figure S3).[6,7] The K_d^{OP} and K_d^{TP} values for Ca^{2+} are 90 ± 2 μM and 89 ± 3 μM, respectively, which are well within the range of $[Ca^{2+}]_m$ in the live cells. We also measured the dissociation constant K_d^i in digitonin-treated HeLa cells by TPM. The value of $K_d^i = 78 \pm 5$ μM is almost the same as that measured in the raft mixture and is well within the range of $[Ca^{2+}]_m$ in live cells. A similar value was reported for Calcium Green FlAsH (CaGF).[8] This result confirms that BCaM is capable of detecting $[Ca^{2+}]_m$ in live cells.

BCaM showed a weak response toward Mg^{2+} at 2 mM, and to Zn^{2+} and Mn^{2+} at 100 μM, and no response toward Fe^{2+}, Cu^{2+}, and Co^{2+} at 100 μM (Supporting Information, Figure S4a). Therefore, this probe can selectively detect near-membrane Ca^{2+} ions with minimal interference from other biologically relevant cations. Moreover, BCaM is pH-insensitive in the biologically relevant pH range (Supporting Information, Figure S4b).

The TP action spectra of BCaM in MOPS buffer containing excess Ca^{2+} indicated a $\Phi\delta$ value of 150 GM at 780 nm, a value that exceeded those of Calcium Green/Ca^{2+} and Fura-2/Ca^{2+} by a factor of three to five (Figure 1c; Supporting Information, Table S1).[6] Thus, TPM images of the cells stained with BCaM would be much brighter than those stained with the commercial probes.

To test whether BCaM can detect near-membrane Ca^{2+}, we have determined the TPEF spectra of BCaM in large unilamellar vesicles (LUVs) composed of 1,2-dipalmitoyl-*sn*-glycero-3-phosphocholine/cholesterol (DPPC)/40 mol% cholesterol (CHL), DOPC/sphingomyelin/CHL (1:1:1, raft mixture), and 1,2-dioleoyl-*sn*-glycero-3-phosphocholine (DOPC) in the presence of excess Ca^{2+}. It is well-established that the cell membrane is composed of liquid-ordered (l_o) and liquid-disordered (l_d) domains, and DPPC/CHL, DOPC, and the raft mixture are good models for the l_o domain, the l_d domain, and the cell membrane, respectively.[9,10] The K_d^{OP} value measured in the raft mixture was 81 ± 4 μM, a value slightly smaller than that measured in the MOPS buffer (Figure 1b; Supporting Information, Figure S5). This difference can be attributed to the more hydrophobic environment within the vesicles, which would stabilize the BCaM/Ca^{2+} complex and shift the equilibrium toward the formation of the complex. Moreover, the emission spectrum of the BCaM/Ca^{2+} complex showed λ_{max} values at 436 and 452 nm in DPPC/CHL and DOPC, respectively, whereas that in the raft mixture exhibited λ_{max} at 450 nm, which could be fitted to two Gaussian functions centered at 436 and 467 nm, respectively (Supporting Information, Figure S6a); the emission from the BCaM/Ca^{2+} complex in the raft mixture can reasonably reflect those from the l_o and l_d domains. Thus, BCaM is suitable for the detection of Ca^{2+} in the model membrane.

The pseudo-colored TPM image of HeLa cells labeled with 0.5 μM BCaM clearly revealed the Ca^{2+} distribution in the plasma membrane (Figure 2a). It is worth noting that

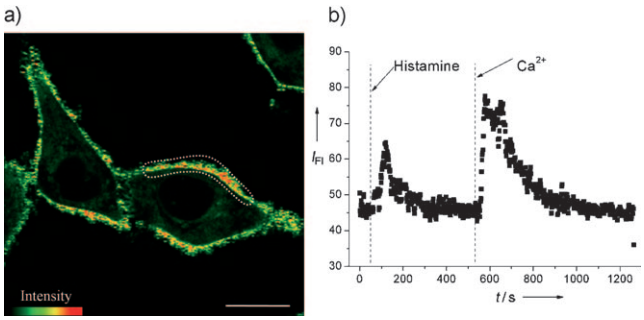

Figure 2. a) Pseudo colored two-photon microscopy (TPM) images of HeLa cells labeled with 0.5 μM BCaM. Scale bar: 20 μm. b) Time course of two-photon excited fluorescence (TPEF) at the position marked with a dotted line in (a) after stimulation with 100 μM histamine in nominally calcium-ion-free buffer, followed by addition of 2 mM $CaCl_2$ to the imaging solution. TPEF was collected at 390–450 nm upon excitation at 780 nm.

BCaM can exclusively stain the plasma membrane despite the absence of the long-chain alkyl group, which is common in most membrane TP probes such as CL.[10] The image was bright, which is probably due to the large TP action cross-section. Also, there were very bright domains (red spots) in addition to the less bright ones, indicating the existence of Ca^{2+}-rich domains in the plasma membrane. Moreover, the

TPEF spectrum from the plasma membrane showed a λ_{max} at 430 nm with a shoulder that could be fitted to two Gaussian functions centered at 430 and 460 nm, respectively, as measured in the raft mixture (Supporting Information, Figure S6a,b). Thus, the TPM image can most reasonably be attributed to the BCaM/Ca^{2+} complexes associated with l_o and l_d domains in the plasma membrane. Moreover, the TPEF intensity in four individual BCaM-labeled HeLa cells chosen without bias remained nearly the same for about 1 h, indicating high photostability (Supporting Information, Figure S7). The combined results confirm that BCaM can detect $[Ca^{2+}]_m$ in live cells for a long period of time. Further, the HeLa cells labeled with BCaM and ANa1 emitted bright TPEF at 390–450 (Ch1) and 500–560 nm (Ch2), respectively (Supporting Information, Figure S8). Therefore, we have selectively detected $[Ca^{2+}]_m$ and $[Na^+]_i$ by using the detection windows of 390–450 (Ch1) and 500–560 nm (Ch2), respectively.

To demonstrate the utility of this probe in cell imaging, we monitored TPEF intensity of HeLa cells labeled with BCaM after addition of histamine, an agonist that stimulates the cells to release $[Ca^{2+}]_c$ from intracellular stores, such as endoplasmic reticulum (ER).[11] We expected that the excess $[Ca^{2+}]_c$ liberated by histamine would be extruded from the cell by the cell membrane to maintain the Ca^{2+} homeostasis, thereby increasing the $[Ca^{2+}]_m$.[11] Indeed, the TPEF intensities in the cell membrane began to rise after addition of histamine (100 μM), reached the peak value after 30 s, and returned to the baseline level after 150 s. When the cells were treated with 2 mM $CaCl_2$, the $[Ca^{2+}]_m$ increased immediately, reached a maximum after 50 s, and then decreased to the baseline level after 6.5 min, which concurred with literature results (Figure 2b).[11] Therefore, BCaM is clearly capable of monitoring the change in $[Ca^{2+}]_m$ in live cells over a long time period.

We then investigated Na^+/Ca^{2+} exchange with BCaM in live cells. It is well-established that $[Ca^{2+}]_c$ is strictly maintained by many cellular functions, including the Na^+/Ca^{2+} exchangers (NCX), which transport one Ca^{2+} out of the cell and take three Na^+ into the cell.[2,3] To visualize such activity, we have monitored TPM images of HeLa cells co-labeled with BCaM and ANa1 (Figure 3a–e). When the cells were treated with histamine (100 μM), the TPEF intensities in the plasma membrane (Figure 3e, position 1, green curve) and cytoplasm (Figure 3e, position 2, red curve) increased sharply until they reached the peak intensities and then decreased slowly to the baseline level. The rates were faster in the plasma membrane than in the cytoplasm, indicating that Na^+ influx occurred after Ca^{2+} efflux through the NCX in the plasma membrane.[12] Therefore, BCaM, in combination with ANa1, is clearly capable of monitoring Na^+/Ca^{2+} exchange.

We further investigated the utility of this probe in tissue imaging. TPM images were obtained from a slice of fresh rat hippocampal tissue incubated with 10 μM BCaM and 20 μM ANa1 for 30 min at 37 °C. The slice from the brain of a 14-day-old rat was too large to show with one image, so two images were obtained in each plane and combined. The bright-field image revealed the CA1 and CA3 regions and also the dentate gyrus (DG; Figure 3f). As the structure of the brain tissue is known to be inhomogeneous in its entire

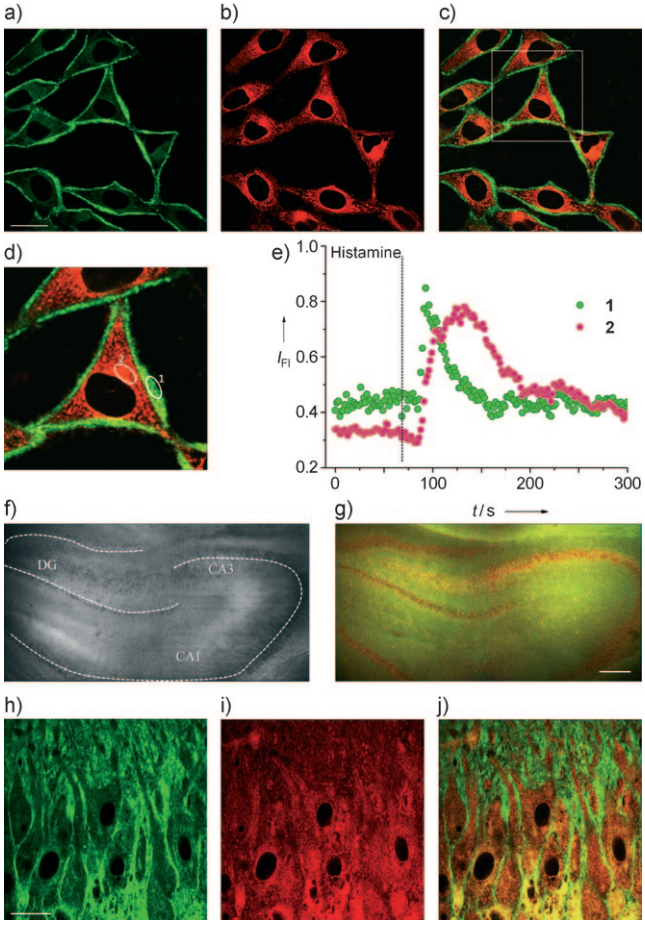

Figure 3. a–e) Dual-channel TPM images of HeLa cells co-labeled with BCaM and ANa1 collected at a) 390–450 nm (BCaM, Ch1) and b) 500–560 nm (ANa1, Ch2). c) Merged image of (a) and (b); d) enlargement of the white box in (c). e) Time course of TPEF at designated positions (1) and (2) in (d) after stimulation with 100 μM histamine in nominally calcium-ion-free buffer. f–j) Images of a rat hippocampal slice co-stained with BCaM and ANa1. f) Bright-field image of the CA1-CA3 regions and the dentate gyrus (DG) at tenfold magnification. g) 25 TPM images collected at Ch1 and Ch2 in (f) along the *z* direction at the depths of approximately 100–200 μm were accumulated and then merged. h–j) TPM images of CA3 regions collected at h) Ch1 and i) Ch2 at a depth of about 100 μm at tenfold magnification. j) Merged image of (h) and (i). Excitation wavelength: 780 nm. Scale bars: 30 μm (a,h) and 300 μm (g).

depth, we accumulated 25 TPM images at depths of 100–200 μm to visualize the distributions of the Ca^{2+} and Na^+ ions (Figure 3g; Supporting Information, Figure S9).

The TPM images collected from Ch1 and Ch2 revealed the Ca^{2+} and Na^+ distributions, which did not merge (Figure 3g–j; Supporting Information, Figure S9b–d). This outcome confirms that BCaM and ANa1 can independently detect $[Ca^{2+}]_m$ and $[Na^+]_i$ with minimum interference from each other. The images taken at a higher magnification at a tissue depth of about 100 μm clearly revealed Na^+/Ca^{2+} distribution in the pyramidal neuron layer composed of cell bodies in the CA3 region (Figure 3h–j). Thus, dual-channel imaging of $[Ca^{2+}]_m$ and $[Na^+]_i$ is clearly possible at a 100–200 μm depth in live tissues by TPM using BCaM and ANa1 as the probes.

In conclusion, we have developed a TP probe (BCaM) that shows a 14-fold TPEF enhancement in response to Ca^{2+}, dissociation constant (K_d^i) of 78 ± 2 μM, high sensitivity and selectivity for $[Ca^{2+}]_m$, and TPEF emission that was three times stronger than Calcium Green and Fura-2 upon complexation with Ca^{2+}. BCaM, which is superior to currently available probes, in combination with ANa1 allows dual-color imaging of the activities of near membrane Ca^{2+} and cytosolic free Na^+ ions in live cells and tissues at depths of over 100 μm for long periods of time without photobleaching artifacts.

Received: May 14, 2010
Published online: August 16, 2010

Keywords: calcium · fluorescence spectroscopy · imaging agents · live tissue · two-photon microscopy

[1] M. J. Berridge, M. D. Bootman, H. L. Roderick, *Nat. Rev. Mol. Cell Biol.* **2003**, *4*, 517.
[2] R. Rizzuto, T. Pozzan, *Physiol. Rev.* **2006**, *86*, 369.
[3] M. P. Blaustein, W. J. Lederer, *Physiol. Rev.* **1999**, *79*, 763.
[4] a) W. R. Zipfel, R. M. Williams, W. W. Webb, *Nat. Biotechnol.* **2003**, *21*, 1369; b) F. Helmchen, W. Denk, *Nat. Methods* **2005**, *2*, 932.
[5] H. M. Kim, B. R. Cho, *Acc. Chem. Res.* **2009**, *42*, 863.
[6] a) P. S. Mohan, C. S. Lim, Y. S. Tian, W. Y. Roh, J. H. Lee, B. R. Cho, *Chem. Commun.* **2009**, 5365; b) Y. N. Shin, C. S. Lim, Y. S. Tian, W. Y. No, B. R. Cho, *Bull. Korean Chem. Soc.* **2010**, *31*, 599.
[7] M. K. Kim, C. S. Lim, J. T. Hong, J. H. Han, H. Y. Jang, H. M. Kim, B. R. Cho, *Angew. Chem.* **2010**, *122*, 374; *Angew. Chem. Int. Ed.* **2010**, *49*, 364.
[8] O. Tour, S. R. Adams, R. A. Kerr, R. M. Meijer, T. J. Sejnowski, R. W. Tsien, R. Y. Tsien, *Nat. Chem. Biol.* **2007**, *3*, 423.
[9] a) K. Simons, E. Ikonen, *Nature* **1997**, *387*, 569–572; b) K. Simons, D. Toomre, *Nat. Immunol. Nat. Rev. Mol. Cell. Biol.* **2000**, *1*, 31.
[10] H. M. Kim, B. R. Kim, H.-J. Choo, Y.-G. Ko, S.-J. Jeon, C. H. Kim, T. Joo, B. R. Cho, *ChemBioChem* **2008**, *9*, 2830.
[11] a) S. Lin, K. A. Fagan, K. X. Li, P. W. Shaul, D. M. Cooper, D. M. Rodman, *J. Biol. Chem.* **2000**, *275*, 17979; b) T. Nagai, S. Yamada, T. Tominaga, M. Ichikawa, A. Miyawaki, *Proc. Natl. Acad. Sci. USA* **2004**, *101*, 10554.
[12] H. Houchi, K. Kitamura, K. Minakuchi, Y. Ishimura, M. Okuno, T. Ohuchi, M. Oka, *Neurosci. Lett.* **1994**, *180*, 281.

